The structure and dynamics of patterns of Benard convection cells

1992 J. Phys.: Condens. Matter 4 931

(http://iopscience.iop.org/0953-8984/4/4/004)

J. Phys.: Condens. Matter 4 (1992) 931–943. Printed in the UK

The structure and dynamics of patterns of Bénard convection cells

N Rivier†

Institut de Physique Expérimentale, Université de Lausanne, CH-1015 Dorigny-Lausanne, Switzerland and
MSD 223, Argonne National Laboratory, Argonne, IL 60439, USA

Received 18 March 1991, in final form 29 September 1991

Abstract. Bénard–Marangoni convection, in containers with large aspect ratio, exhibits space-filling cellular structures, highly deformable, but crystallized. They contain dislocations and grain boundaries generated and moved by elementary topological transformations, and are subjected to a weak shear stress due to the earth's rotation. The cellular structure and its fluctuations are analysed from a crystallographic viewpoint, by using two complementary approaches. One is a global analysis of cellular structures in cylindrical symmetry. Their structural stability and defect pattern are obtained as topological mode-locking of a continuous structural parameter. The other, a local, molecular dynamics of the cells, gives a realistic parametrization of the forces and the transformations by generalizing the Voronoi cell construction in one extra dimension.

1. Introduction. Topological representation of hydrodynamic patterns

This is an attempt to solve a structural problem of hydrodynamics by using crystallographic methods and concepts, in terms of cells, topological defects like dislocations, their interaction and their motion. Conversely, it can be read as an application of crystallography to extremely soft and deformable, albeit crystalline materials. Such materials are known to exist: colloidal crystals [1], bubble rafts [2], magnetic bubbles [3], etc.

Here, we shall investigate the cellular structure produced by Bénard–Marangoni [4] convection. A fluid heated from below exhibits convection motion above a certain temperature threshold. The hotter fluid rises by buoyancy, and is drawn towards the colder regions of the (upper) free surface by their stronger surface tension, where it goes down. When the size of the container is much larger than the thickness of the fluid (approximately the cell size), one observes a two-dimensional cellular pattern (a froth). On the free surface, the fluid propagates from the hotter cell centres to the colder vertices of the froth.

Hot points repel each other like soft disks. Some cells divide. Just above the convection threshold, the structure is ordered (one recognizes reticular planes, dislocations, etc), and one anticipates a perfect hexagonal structure (triangular packing of repelling disks) for the ground state, as was indeed pointed out by Bénard himself [5].

† Permanent address: Blackett Laboratory, Imperial College, London SW7, UK.

0953-8984/92/040931+13$04.50

However, this perfect hexagonal structure is never observed when the upper surface of the fluid is free (Bénard–Marangoni convection)†:

(i) There are always defects (pentagonal and heptagonal cells), well in excess of the 6 pentagons required by topology‡

(ii) The whole structure rotates, with the period of Foucault's pendulum [7]. Moreover, the trajectory of the centre of an individual cell is an outgoing spiral [7], suggesting that energy is dissipated outwards from the middle of the container, where new cells are formed. This indicates that cellular structure and individual cells are sheared by the earth's rotation, through the Coriolis force acting on the free (upper) surface of the moving fluid§.

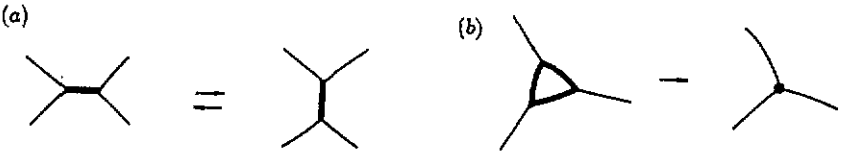

Figure 1. Elementary topological transformations: (*a*) Neighbour switch (T1). (*b*) Cell disappearance (T2).

Dissipation of shear in crystals is carried naturally by dislocations gliding along planes. Cylindrical symmetry, imposed by Coriolis forces and by the shape of the container, should make dislocations align and glide on concentric circles. An indirect proof of the presence of dislocations is the observation that, while the cell rotates about itself with the period of Foucault's pendulum, it undergoes sudden jogs of approximately $2\pi/5$ (when the spiral trajectory intersects a glide circle) [7].

Toplogical defects, dislocations gliding to dissipate shear strain, are crystallographic concepts. All these features are manifest in the convective cell structures,

† I have been informed by one of the referees that perfect hexagonal cellular patterns have been obtained in [6]. Now Bodenschatz *et al* do not claim perfect hexagonal order in their abstract (the only data published), which postdates the redaction of this paper. Ciliberto, Pampaloni and Pérez-García obtain defect-free hexagonal patterns (figure 1 of reference [6b]). However, both these experiments [6] are made under very different boundary conditions (Rayleigh–Bénard instability: fluid bounded below and above by rigid, thermally conducting plates) from those at Marseille [7] (free upper surface of the fluid: Bénard–Marangoni instability, driven chiefly by surface tension inhomogeneities at the free surface, as suggested by Bénard in his original paper, and confirmed by gravity-free experiments in Apollo XIV and XVII spaceships [4]). It is well known that the pattern morphology and stability are different in both cases [4]. Notably, unlike Bénard–Marangoni's, Rayleigh–Bénard convection patterns (rolls, squares or hexagons) can be defect-free (cf figures 6 and 8 of reference [4a], and figure 8 of reference [4b]). Also, the patterns in [6] are not sheared (they are not even rotating as far as I know); once selected, their direction is fixed in the closed container. There is no need for dislocations, except to alleviate the frustration imposed by cylindrical symmetry. This is done by boundaries between hexagonal and rolls patterns (figure 1 of reference [6b]). Contrast this with [7] where the pattern is under shear and rotating with respect to the container. See footnote§.

It is also true that the Foucault period of the structure was proposed with a question mark in the title [7]. The question mark was requested by the referee and the authors were happy to comply (Pantaloni J, private communication). But there can be no doubt that the structure is sheared: See figures 2, 4 and 5 of reference [7], and footnote§.

‡ The free surface of a fluid inside a cylindrical container is topologically equivalent to a half-sphere.

§ Recall that the Foucault pendulum is not rotating in the inertial frame, so that its direction of oscillation rotates in the non-inertial (laboratory) frame with an angular velocity equal and opposite to that of the frame itself. Accordingly, the cellular structure, if uncoupled to the container, would rotate as a whole

except the glide circles which have yet to be observed. We can therefore translate a problem of pattern formation and stability in hydrodynamics (described by hydrodynamic field equations which are complicated to write down and to solve) into a much simpler many-body problem. The bodies are discrete objects (the cells), which repel each other. We want to describe the ground state and elementary excitations. This is a standard problem in crystallography, but here we have (a) cylindrical symmetry, (b) a very soft (deformable, malleable) structure; (b) implies that topological defects can be created and moved easily, while (a) imposes the presence of these defects. The ground state must be structurally stable, i.e. invariant under small fluctuations of its parameters [10].

The basis for the work presented here is the description of the structure and evolution of cellular networks (froths, tissues or foams) and of their evolution. This topological, or many-body analysis of a structure and its defects is a well established technique in froths [11]. Application of these ideas to describe Bénard cellular networks started in the early 1980s, essentially in the Marseille group ([7, 8, 12, 13] and references therein) but it is still fairly controversial, as the author has discovered, essentially because it by-passes the standard, continuous hydrodynamic equations to investigate the stability and structure of interacting, space-filling entities (the cells). Our first paper [10] appeared in 1984, but there has been considerable, recent progress on the structure alone to justify another look. On the other hand, the transposition of the techniques and ideas in the evolution of cellular networks and froths [14] to describe the *dynamics* of Bénard networks is new, and is likely to be challenging, even if only sketchy in this paper. This paper was presented as a poster at the IUTAM symposium on Fluid Mechanics of Stirring and Mixing, La Jolla, CA, August 1990, and has appeared as an abstract in the proceedings [15].

with the period of Foucault's pendulum (approximately 36 h in Marseille (latitude $\simeq 42°$ N)). The trajectory of an individual cell would be a circle in the non-inertial frame. There would be no shear.

Experimentally, there is a flow of energy from the centre to the rim of the container, which is strongest if the rim is made of thermally insulating material, and weakest if it is a metal in thermal contact with the heating plate. This gives rise to a radial component of the motion of every individual cell, whose trajectory is now a spiral, as observed [7]. The combination of circular and radial motions implies that the structure is subjected to shear.

Suppose the equation of motion for the centre of a cell r to be that of a spiral,

$$\mathrm{d}r/\mathrm{d}t = \omega \wedge r + \mathrm{a}(|r|)r. \tag{9}$$

(with a possible dependence of ω on $|r|$). Consider a (locally hexagonal) lattice of these cells. If the strain tensor associated with displacement of the cells within the time interval $\mathrm{d}t$ is equal to $\mu(r)\delta_{ij}$, then the structure is not sheared by the motion. This is the case if and only if the transformation $r(t) \to r(t + \mathrm{d}t)$ is conformal (i.e. it is represented by an analytic function in the complex plane $\{r\}$. *Cauchy–Riemann relations make the off-diagonal element of the strain tensor vanish*). In a spiral lattice (9), absence of shear requires $a = cst$, independent of $|r|$. This constant can be either $a = 0$ (no radial dissipation of energy, circular cell trajectories), or $a \neq 0$, with a logarithmic spiral for the cell trajectory. The spiral lattice is, topologically, perfectly hexagonal (the coordinates of its cell centres given by the complex variable w, can be obtained from a regular hexagonal lattice (z) by the conformal transformation $w = A\exp(-ibz)$, where A and b are constants [8, 9]), but the cell sizes increase outwards. There are no defects, and no grain boundaries. A spiral lattice of equal-sized cells requires circular grain boundaries, on which the transformation $w(z)$ is not conformal, and which are accordingly loci of shear strain.

2. Elementary topological transformations

Structural defects are created and moved by elementary topological transformations [11]. Consider a two-dimensional cellular froth with C cells, separated by E edges or interfaces, meeting at V vertices. E and V are secondary, topological elements partitioning space between the physical hot points C. Edges are free to expand or shrink at the mercy of the motion of the hot points, leaving the structure topologically invariant until one of them disappears, inducing an elementary topological transformation (ETT) (figure 1). There are only two types of ETT, neighbour switching (T1), or cell disappearance (T2), and its inverse. Cellular division or mitosis (the topological agent of growth of biological tissues), is the composition of $(T2)^{-1}$ with a few T1. It is observed, for example, on Lake Natron [16] a soda lake in Tanzania, and in the process of formation of Bénard–Marangoni cellular structures.

Vertices are tri-valent (coordination $z = 3$) except at the critical point of a T1 transformation, a 'Four-corner Boundary'. Not only structural stability, but also dynamics imposes $z = 3$. Repelling hot points triangulate space, which is partitioned, for example, by drawing perpendicular bisectors. The three bisectors (E) of a triangle meet at a point (V), which is $z = 3$.

Euler's identity [11],

$$C - E + V = 1 \tag{1}$$

for a finite planar cellular froth (the cell at ∞ is not included), and valencies relations, $zV = 2E$, $\langle n \rangle C = 2E$ (each edge joins 2, $z = 3$-valent vertices, and separates 2 cells, $\langle n \rangle$-sided on average), imply that

$$\langle n \rangle = 6 - (\text{boundary corrections}). \tag{2}$$

Nearly all cells are hexagonal, as observed by Bénard [5]. Also, $6C = 2E = 3V$.

ETT change the number of sides of the cells involved in the transformation. A five- (respectively seven-) sided cell is a positive (negative) disclination. (A pentagon is produced in a hexagonal lattice by cutting out a $2\pi/5$ wedge and re-glueing. The plane buckles into a cone, and the pentagon is a source of positive curvature. Similarly, a heptagon is produced by adding a wedge, and is a source of negative curvature. The plane buckles into a saddle.)

A dipole pentagon–heptagon is a dislocation (figure 2) (produced by cutting out a rectangular strip, and re-glueing. The plane remains flat—uncurved—but it has a step. The source of the step is the dislocation). A single T1 in a hexagonal froth generates a pair of dislocations, which glide apart upon applying shear stress, by successive T1, i.e. by a purely *local* process. Similarly, one single cell division (figure 3) generates a pair of dislocations. Further divisions in the neighbouring cells make the two dislocations climb away from each other like a defective zipper, leaving behind a layer of new cells. Again, this is a *local* means of adding material (unlike the cutting scenario above). It is the way that our intestine grows [17].

ETT are local transformations, which, like collisions in gases, keep the cellular network in statistical equilibrium. The observable manifestation of this local balance is given by Aboav's relation [11, 18].

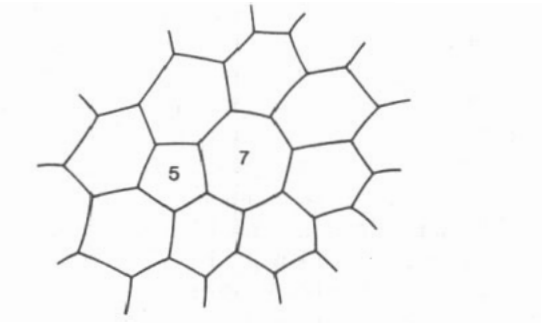

Figure 2. Topological dislocation (pentagon–heptagon pair).

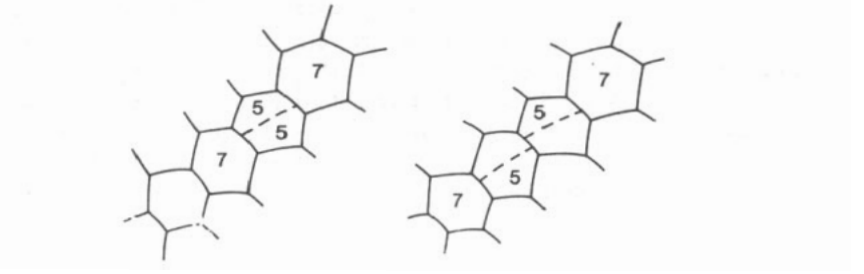

Figure 3. Creation and climb of a dislocation pair by successive cell divisions.

3. The DAISY, ideal crystal in cylindrical symmetry [8]

The ideal, infinite $z = 3$, planar crystal is a perfect hexagonal lattice. It does not have cylindrical symmetry. The ideal, $z = 3$ crystal with cylindrical symmetry is the DAISY, shown in figure 4. It is a computer construction (by a single algorithm given in equation (3)) of the structure of several *compositae* (composite flowers like daisies, asters, etc), which is indeed cylindrical and crystallographic ('atoms' are identical, $s = 1, 2, \ldots$ florets, sprouting from a central stem and pushing out their elder brothers, labelled by larger s) [10, 19].

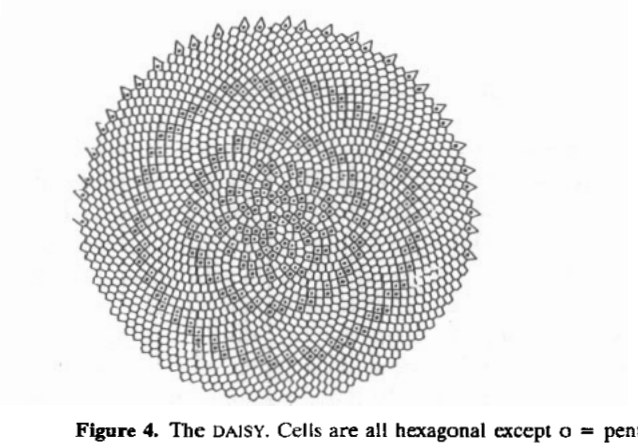

Figure 4. The DAISY. Cells are all hexagonal except o = pentagon, + = heptagon, dipole o+ = dislocation. Grain boundaries are quasi-crystalline. (From reference [10]).

One notices immediately concentric circles of dislocations (dipoles 5/7) which are the glide circles necessary to dissipate shear. They are boundaries between perfect, hexagonal grains. It is well known that grain boundaries are array of dislocations. But here, the array is quasi-periodic [20]. The perfect, hexagonal grains have reticular 'planes' which are the visible spirals or parastichies in composite flowers. All but a few percent of *compositae* have Fibonacci numbers of spirals $1,1,2,3,5,8,13,21,34\ldots$ and the remaining few follow the similar Lucas sequence $1,3,4,7,11,18,29\ldots$. (The outer grains have higher numbers than the inner ones, running through the sequence in an automatic and self-similar fashion [8, 10, 19].) We have therefore a cylindrical cellular structure which is topologically stable (section 4) and universal (Fibonacci and Lucas sequences). This universality, noted by Leonardo, Kepler, Goethe ..., remains the major outstanding puzzle of phyllotaxis (plant architecture) [8, 19, 21].

Two-dimensional phase transitions (e.g. melting) are mediated by the unbinding of pairs of topological defects, dislocations (or vortices) and, possibly, disclinations [12]. A representation (figure 4) of the ground state structure, emphasizing the position and function of topological defects, is a prerequisite to understanding the Bénard–Marangoni structures observed experimentally, which have increasing amounts of disorder as the temperature increases above threshold. It is easy to melt the structure, harder to pinpoint the transition(s) [13].

4. Structural stability and universality of the DAISY

Fluctuations of a structure can be represented by a dynamical map; universality and stability of the structure are then consequences of universality and stability of dynamical maps.

A crystallographic structure must be *labelled* and described by a *local reference frame*. In conventional, translationally invariant systems, the frame is the fundamental domain or unit cell, and each atom is labelled by the position of its unit cell (i.e. by D integers in D dimension), with, if necessary, an index giving its position within the cell. In cylindrical symmetry, we are limited to one integer $s = 1,2\ldots$, labelling each cell from the centre outwards (from younger to older florets). The cell's centre is then given in cylindrical coordinates by

$$\begin{aligned} \theta(s) &= 2\pi\lambda s \\ r(s) &= \text{monotonic increasing function of } s. \end{aligned} \tag{3}$$

Cells are then drawn by democratic partition of space between centres (Voronoi construction [11]: interfaces are perpendicular bisectors between neighbouring centres, and every point inside a cell is closer to this cell's centre than to any others). This produces the DAISY of figure 4. The structure is parametrized essentially by one quantity, the divergence angle $2\pi\lambda$, $\lambda \in [0,1]$. The cells lie on a generative spiral $r(\theta/2\pi\lambda)$, not visible in figure 4 because successive florets are not neighbours. (The pitch of the generative spiral is smaller than the cell radius.) Only visible are the reticular spirals (parastichies), which are ordered as $\{\lambda s\}$. ($\{n\}$ is the fractional part of n, $n = \{n\}$ modulo 1. The ordering follows from the fact that equation (3), projected on $r = cst$, is a circle map.) A minor adjustment in the function $r(s)$ straightens the spirals while retaining the ordering, glide circles, etc [8].

Neighbours $s, s + B_m$, have appropriately the same azimuth $\theta(s + B_m) \simeq \theta(s)$, and $\lambda \simeq A_m / B_m$. If these were equalities (λ rational), cell centres would lie on the same radii, and the Voronoi cellular structure would resemble a spider's web [10]. λ is therefore irrational, and representable uniquely as a continued fraction,

$$\lambda = 1/\{c_1 + 1/[c_2 + 1/(c_3 + 1/\ldots)]\} \simeq 1/\{c_1 + 1/[\ldots + 1/c_m]\} = A_m/B_m \tag{4}$$

($0 < c_i, A_m, B_m, s \in Z^+$ are natural numbers). A_m / B_m is called the mth convergent to the irrational λ. B_m is the number of cells in a circular shell (one cell thick), or the number of reticular spirals. It labels neighbours. (A_m is the number of turns in the generative spiral necessary to fill the shell.)

An hexagonal cell in a grain has six neighbours, and belongs to three families of reticular spirals. Its neighbours are labelled by three B_ms, denominators of three convergents to λ. Thus the *local reference frame* is the triangle of labelled neighbours $(s+B_m, s+B_{m-1}, s+B_{m-2})$ to a given cell s (figure 5). One goes from s to $s+B_m$ either directly, or jogging through the other two parastichies and the final label must be independent of the path and of the origin cell, $s + B_m = (s + B_{m-2}) + B_{m-1}$, thus,

$$B_m = B_{m-1} + B_{m-2} \tag{5}$$

which is the relation generating Fibonacci, Lucas etc, sequences. The triangular relation (5) is crystallographically central and overriding.

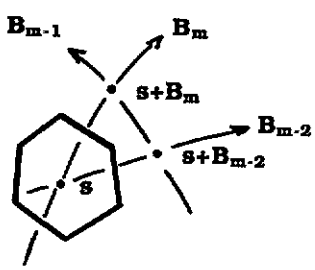

Figure 5. Reference frame, showing labels of cell s and its neighbours, and demonstrating the triangular relation, equation (5).

A grain is characterized by the reference frame $\{B_m, B_{m-1}, B_{m-2}\}$. At a grain boundary, two families of reticular spirals go through, and the third is replaced by a higher B_{m+1} (better convergent), through dislocations which do indeed add material. There are two possibilities [8, 10],

$$\begin{aligned} &\text{(i)}\ \{B_m, B_{m-1}, B_{m-2}\} \rightarrow \{B'_{m+1}, B_m, B_{m-1}\} \qquad \text{regular transition} \\ &\text{(ii)}\ \{B_m, B_{m-1}, B_{m-2}\} \rightarrow \{B''_{m+1}, B_m, B_{m-2}\} \qquad \text{singular transition} \end{aligned} \tag{6}$$

with B'_{m+1} and B''_{m+1} consistent with equation (5). Only the former gives the observed Fibonacci or Lucas phyllotaxis. λ is then *noble* ($\{c_i\} = 1$, $i \geqslant i_0$). Noblest is the golden mean $1/\tau = (1-\sqrt{5})/2$, ($i_0 = 1$), generating the Fibonacci sequence.

The singular transition involves intermediate convergents, $c_i \neq 1$, and non-noble λ [8, 10].

Consider a given grain $\{B_m, B_{m-1}, B_{m-2}\}$, that is, a set of three rational convergents to λ, with A_m/B_m bounded by the other two. It can easily be shown that any $\lambda \in]A_{m-1}/B_{m-1}, A_{m-2}/B_{m-2}[$ generates the same ordering of B_m successive cells or reticular spirals: $s, s + B_{m-2}, s + 2B_{m-2}, \ldots (\mathrm{mod} B_m)$, or $s, s+B_{m-1}, \ldots (\mathrm{mod}\ B_m)$, clockwise or anticlockwise, i.e. the same structure $\{\lambda s\}$. This is a topological mode-locking. The structure is locked on that given by the rational convergent A_m/B_m, for any λ within the interval $]A_{m-1}/B_{m-1}, A_{m-2}/B_{m-2}[$. The possible structures (A_m/B_m) follow an incomplete devil's staircase as a function of λ, exactly as in conventional mode-locking of two coupled oscillators [22] where the abscissa of the staircase represents the ratio of their natural frequencies, and the ordinate, the observed ratio, locked to rationals.

At a grain boundary, it is necessary for the structure to lock on rationals with larger denominators $B_m \rightarrow B_{m+1}$ (6). (Recall that B_m is the number of cells filling a circular shell. This number must increase as one goes outwards, in order to keep the cell size (approximately equal to fluid thickness) constant.) In ordinary mode-locking, the coupled oscillators achieve a finer tuning if instead of locking on p_1/q_1 (one oscillator making p_1 oscillations in q_1 periods of the other, before the two return in phase) or on p_2/q_2, they lock on the new rational frequency,

$$(p_1 + p_2)/(q_1 + q_2) \equiv p_1/q_1 \oplus p_2/q_2 \tag{7}$$

(Farey sum). Note that the denominators $q_1 + q_2 = q_1 \oplus q_2$ satisfy the triangular rule (5). Equation (7) generates and orders all the rationals $\in [0, 1]$ uniquely as in figure 6, the Farey construction [9].

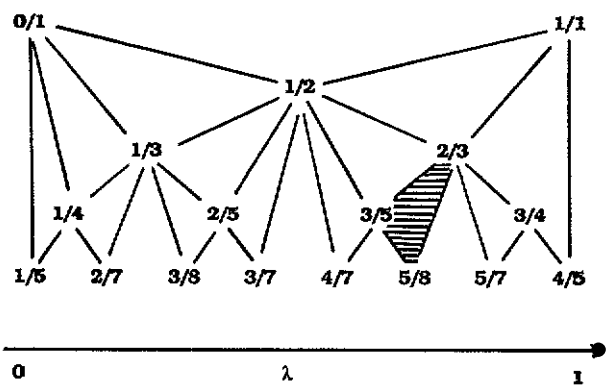

Figure 6. Farey construction of rationals. A triangle defines a grain, structurally locked-in.

Figure 6 can be seen as a tiling by triangles, with a triangle representing grain $\{B_m, B_{m-1}, B_{m-2}\}$. A grain boundary forces a bifurcation. The triangle is replaced by either one of the two Farey offsprings, coinciding with the regular or singular transition of equation (6) (figure 7).

It is easy to introduce a scalar weight measuring the strain necessary to confine λ within the interval yielding the required structure. This weight plays the role of an energy. Structure-conserving fluctuations of λ can be represented generically

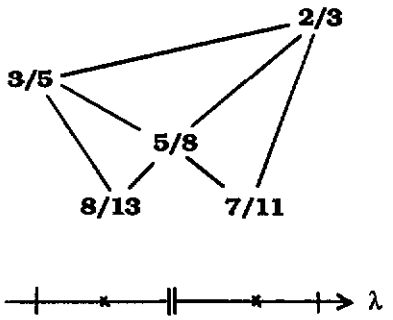

Figure 7. Bifurcation at a grain boundary. Here, the regular transition is on the left (8/13), the singular transition on the right (7/11).

by dynamical maps (sending the interval into itself, with A_m/B_m, and the interval boundaries A_{m-1}/B_{m-1}, and A_{m-2}/B_{m-2} as fixed points), e.g. by homographic functions. Homographic functions with rational fixed points have remarkable properties (they are involutions and the fixed points have marginal stability). The energy necessary to fix the structure is then a simple functional of the fluctuation map, exactly as a Ginzburg–Landau free energy is a function of some order parameter.

An energy can similarly be associated with each alternative E^{ST}, E^{RT} at a bifurcation, and with the operation funnelling a divergence λ from the ST side of a bifurcation into a regular transition (E^F). One finds readily that $E^{RT} < E^F < E^{ST}$ and this is sufficient to justify the universality (and the structural stability) of *compositae*, which always select the lowest energy alternative (RT) at every bifurcation encountered upon growth [21]. This preference has not been tested on Bénard–Marangoni structures as yet.

Either choice at the bifurcation is compatible with the triangular equation (5), and yields a grain boundary sequence of dislocations (D) and isolated hexagons (H). Dislocations are defects, sources of strain which repel each other, and their number is imposed by the convergents B_m of λ. A smooth, quasi-periodic sequence of D and H results [20, 23]. Shear is absorbed by a dislocation glide on this quasi-periodic structure through a T1, as,

$$\ldots \underline{\mathrm{DD}}\mathrm{HDH}\ldots \rightarrow \ldots \mathrm{DH}\underline{\mathrm{D}}\mathrm{DH}\ldots \tag{8}$$

(glide of the underlined dislocation by a cell's diameter). The action is then repeated on another dislocation, as in an ideally efficient, $1/\tau$-full parking lot (D are the cars, H the empty spaces).

This concludes the global description of Bénard–Marangoni structures under shear. We have been able to accommodate structure-conserving fluctuations. The lowest topological excitations are T1 on grain boundaries (8), which dissipate shear efficiently. The next lowest topological excitations are T1 creating new dislocation pairs, at first near the grain boundaries, then within the grains. Next are cellular divisions which create dislocation pairs (figure 3) and additional cells. But, at that level of excitation, one should shift to a local description of the dynamics of cellular structures.

5. Local dynamics of cells

We now discuss the local dynamics of the cellular structure, not as a field theory,

but as a many-body problem where the cells (hot points) are the bodies, interacting through some reasonable repulsive two-body potential. We require that the representation automatically generates a space-filling, cellular froth, and that ETT in the froth correspond to elementary local displacement of the bodies.

A simple generalization of the Voronoi (democratic) partition of space between seeds (hot points) produces a froth with realistic structure (isotropic cells), capable of accommodating T2 or cellular divisions [14, 24, 25]. Consider circles instead of points as seeds, and define the (Laguerre) distance of a point P to a circle Γ (hypersphere in $D > 2$ dimension) as the length of the tangent to Γ through P (power of P with respect to circle Γ). The locus of points at equal distance between two circles is a straight perpendicular line, the radical axis (hyperplane if $D > 2$), which generalizes perpendicular bisector to unequal circles. Like perpendicular bisectors in a triangle, the three radical axes of three circles are concurrent. They are the interfaces of the Laguerre froth. The larger the circle seed, the larger its corresponding cell in the froth. Laguerre froth reduces to Voronoi's if all the seed circles are equal. Small fluctuations in circle radii already generate realistic cell shapes. Generalization to 3 or more dimensions is straightforward, as is the analysis of a section of the froth [24] (itself a Laguerre froth), important in the analysis of 3D polycrystalline aggregates in metallurgy (stereology). The dynamical evolution of the froth is much more manageable than its construction [14].

The radical axis between two circles of radii r_1 and r_2 depends on $r_1^2 - r_2^2$ only. This remark gave Telley [14] the idea of representing seeds as identical, vertical paraboloids (umbrellas) in one extra dimension, which intersect the horizontal, physical space as the Laguerre circles. The altitude of the physical plane is fixed but arbitrary. The umbrellas are the bodies of our problem, each specified by the three coordinates $q = (x, z)$ of their apex. Here, x is the coordinate of the circle's centre in the two-dimensional physical space, and z, the height above physical space, measures the circle radius, $z \sim r^2$, or the cell size.

Now for the ETT. The set of seeds looks like a Yosemite mountain profile (figure 8). A paraboloid below the horizon (a seed too small) does not generate any cell in the froth. Conversely, a paraboloid which is too high (a seed too large) obscures smaller paraboloids nearby and gobbles up their representative cells. So, a T2 topological transformation occurs whenever the z coordinate of a paraboloid is pushed below the horizon. Conversely, when a new paraboloid rises above the horizon, it divides the cell containing its apex. T1 transformations are produced by moving nearby seeds horizontally rather than vertically. ETT are therefore naturally induced by motions of the bodies, T1 by horizontal (x) motion, T2 or cell division by vertical (z) motion.

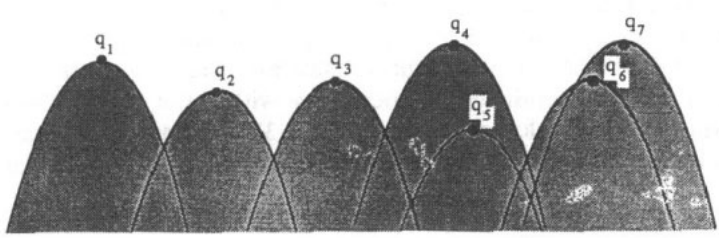

Figure 8. The 'Yosemite' horizon of paraboloid seeds. The horizontal axis represents the physical plane. Seed q_5 is below the horizon and does not generate a cell in the froth. From Telley [14].

There is a duality between cell seed paraboloids (umbrellas) and vertices of Laguerre froth, i.e. between hot and cold points in the convective structure [14]. Vertices can also be represented by the same paraboloid as the cell seeds, but inverted (opening upwards). The bottom $q^* = (x^*, z^*)$ of the inverted paraboloid lies on the intersection of its three adjacent paraboloids. The converse is also true, but more stringent: the umbrella apex q lies on the intersection of its six adjacent, inverted paraboloids. This non-random coincidence indicates clearly the restrictions necessary to produce a froth [14]. Any set of C seeds (bodies) produces a Laguerre froth, specified by $3C$ coordinates (x, z) in two dimensions. But the froth has $V = 2C$ vertices, which would have required $4C$ coordinates if chosen independently. Note that independent orientation only of every interface ($E = 3C$) also gives the required number of degrees of freedom. Physically, edge orientation (crack) may be the relevant degree of freedom in brittle fragmentation or geological jointing processes.

Duality yields the driving forces on the hot points (seeds), if the energy E is proportional to the total interfacial length, as is clearly the case in soap froths (surface tension) and in metallurgical aggregates (grain boundary energy), less obviously so in fluids. Displacement of a seed paraboloid q displaces, geometrically, the nearby vertex paraboloids q^*, hence changes the interfacial length and the energy of the froth. This produces a force $F = -\nabla_q E$ on q. Neighbouring seeds are fixed, so that only the n-sided central cell q is deformed, with its vertices sliding on the fixed incident interfaces (n degrees of freedom to minimize the energy cost of moving q.

Laguerre's froth, with paraboloid seeds [14] constitutes therefore an excellent model for understanding and simulating the dynamics of a cellular structure. It identifies the independent degrees of freedom (cells, hot points in one extra dimension), generates elementary topological transformation by simple, local motion, and computes the forces by a realistic, local geometric algorithm. In a cylindrical container, it should relax to the DAISY ground state of section 4, even in the limit of negligible shear, but this remains to be tested.

6. Conclusions

A crystallographic representation of cellular convective structures in cylindrical symmetry or under shear has been presented. The 'atoms' are the hot points, cells of the froth. Structural integrity is only disturbed by elementary topological transformations. ETT generate structural defects (pairs of dislocations) and make them move (glide by T1, climb by cellular division). Global (ground state structure, dislocation glide on grain boundaries), and local (Laguerre–Telley modelling of the cellular structure) analyses of the structure, its stability and its dynamics have been presented.

Two tests remain to be carried out:

(i) To obtain experimentally DAISY as the structure taken up by Bénard–Marangoni convection at a higher rate of shear.

(ii) To combine global and local analyses, by calculating the ground state of the Laguerre froth in cylindrical symmetry, or by melting the DAISY through thermal fluctuations under Laguerre–Telley dynamics. (This was done in reference [10] by imposing random fluctuations of the cell's seeds position x only, neglecting forces.)

The experimental status, as of June 1991, in so far as I am aware, is as follows:

(i) Full alignment of dislocations on circles has not been observed under weak shear due to the earth's Coriolis force, and not yet under a higher rate of shear (M Howald and R Huguenin (Lausanne), private communication, C Boon (Imperial College), private communcation). Here, we face a technical problem. The structure is not sheared in the two extreme situations, either if it is locked to the rotating container (if the walls are rough or the heating inhomogeneous, as in Boon's experiment), or if, conversely, it remains stationary (apart from the earth's Coriolis effect) with respect to the laboratory while the container is rotating, like the Foucault pendulum to a galactic observer. By contrast, the Marseille [7] and Lausanne structures rotate with respect to the container and the laboratory, and may well be the optimal situation where shear is maximized. (See footnote§.)

(ii) Telley [14] did successfully simulate the dynamics of polycrystalline aggregates (sintering process). Some analytical results have been obtained [26]. But this has yet to be applied to Bénard convection cells.

(iii) Noever [27] has shown recently that colonies of protozoa exhibited cellular patterns due to Rayleigh–Taylor instability. They have been studied under varying gravity field, but not yet in rotation.

(iv) The dynamics of a single topological defect, and the interaction between two defects in a fluid described by a complex Ginzburg–Landau equation, has recently been studied experimentally, theoretically and in simulations [28]. These studies show that a topological defect is a valid concept and dynamical object, but do not shed light on the spatial organization of many defects in a frustrated (and sheared) situation.

Acknowledgments

Suggestions from and discussions with R Occelli, J Pantaloni, R Blanc, A J Koch, F Rothen, H Telley, A Mocellin, M Howald, R Huguenin, C Boon, D Weaire and the referees are gratefully acknowledged, as is hospitality in Marseille (Université de Provence, Laboratoire de Dynamique des Fluides) in 1982, and Lausanne (Institut de Physique Expérimentale de l'Université) in 1990. Work at Argonne is supported by US DOE contract W-31-109-ENG-38; work in Lausanne, by a grant from the Herbette Foundation.

References

[1] Pieranski P 1983 *Contemp. Phys.* **24** 25
Joanicot M, Jorand M, Pieranski P and Rothen F 1984 *J. Physique* **45** 1413
[2] Bragg W L and Nye J F 1947 *Proc. R. Soc.* A **190** 474
Georges J M, Meille G, Loubet J L and Tolen A M 1986 *Nature* **320** 342
[3] Howell P R, Kilvington I T, Willoughby A and Ralph B 1974 *J. Mater. Sci.* **9** 1823
Molho P 1988 private communication
Babcock K L and Westervelt R M 1989 *Phys. Rev.* A **40** 2022
[4] (a) Normand C, Pomeau Y and Velarde M G 1977 *Rev. Mod. Phys.* **49** 581
(b) Bergé P and Dubois M 1984 *Contemp. Phys.* **25** 535
(c) Busse F H 1978 *Rep. Prog. Phys.* **41** 1931
[5] Bénard H 1900 *Rev. Gén. Sci. Pures et Appl.* **11** 1261, 1309
[6] (a) Bodenschatz E, de Bruyn J, Ahlers G and Cannell D S 1991 *Bull. Amer. Phys. Soc.* **36** 653
(b) Ciliberto S, Pampaloni E and Pérez-García C 1991 *Phys. Rev. Lett.* **61** 1198

[7] **Pantaloni J**, Cerisier P, Bailleux R and Gerbaud C 1981 *J. Physique Lett.* **42** L147
[8] Rothen F and Koch A J 1989 *J. Physique* **50** 633
[9] Coxeter H S M 1961 *Introduction to Geometry* (New York: Wiley)
[10] Rivier N, Occelli R, Pantaloni J and Lissowski A 1984 *J. Physique* **45** 49
Occelli R 1985 Transitions ordre–désordre dans les structures convectives bi-dimensionelles *Thesis* Université de Provence, Marseille
[11] Weaire D and Rivier N 1984 *Contemp. Phys.* **25** 59
[12] Kosterlitz J M and Thouless D J 1978 *Prog. Low Temp. Phys.* 7 B 371
Nelson D R and Halperin B I 1979 *Phys. Rev.* B **19** 2457
[13] Occelli R, Guazelli E and Pantaloni J 1983 *J. Physique Lett.* **44** L597
[14] Telley H 1989 Modélisation et simulation de la croissance des mosaiques polycristallines *Thesis* EPFL, Lausanne, Switzerland
[15] Rivier N 1991 *Phys. Fluids* A **3** 1467
[16] Krafft K and Krafft M 1981 *Dans l'Antre du Diable* (Paris: Presses de la Cité) p 53
[17] Pyshnov M B 1980 *J. Theor. Biol.* **87** 189
[18] Aref H and Herdtle T 1990 *Topological Fluid Mechanics (Proc. IUTAM Symposium)* ed H K Moffatt and A Tsinober (Cambridge: Cambridge University Press) pp 745–64
Blanc M and Mocellin A 1979 *Acta Met.* 27 1231
Rivier N 1985 *Phil. Mag.* B **52** 795
[19] Rivier N 1988 *Mod. Phys. Lett.* B **2** 953
[20] Rivier N 1986 *J. Physique Coll.* **47** C3 299
[21] Rivier N, Koch A J and Rothen F 1991 *Biologically Inspired Physics* ed L Peliti and S Leibler (New York: Plenum)
[22] Pippard A B 1978, 1989 *The Physics of Vibration* vol II (Cambridge: Cambridge University Press) pp 391–413
Baums D, Elsässer W and Göbel E O 1989 *Phys. Rev. Lett.* **63** 155
[23] Rivier N and Lawrence A J A 1988 *Physica* B **150** 190
[24] Imai H, Iri M and Murota K 1985 *SIAM J. Comput.* **14** 93
[25] Aurenhammer F 1987 *SIAM J. Comput.* **16** 78
[26] Rivier N 1990 *J. Physique Coll.* **51** C7-309; 1991 *Comptes Rendus Acad. Sci.*
[27] Noever D 1991 *Phys. Rev.* A **44** 5279
[28] Goren G, Procaccia I, Rasenat S and Steinberg V 1989 *Phys. Rev. Lett.* **63** 1237
Rica S and Tirapegui E 1990 *Phys. Rev. Lett.* **64** 878